Influence of welding conditions on the fatigue behaviour of spot welds

Frédérique Rossillon[a], André Galtier, Jean-Louis Robert[b], Arnaud Lens[a], Michel Duchet[a], H. Oikawa[c]

[a] Arcelor Research, Voie Romaine, BP 30320, 57283 Maizières-les-Metz, France
[b] LaMI, IUT de Montluçon, BP 2235, 03101 Montluçon Cedex, France
[c] Nippon Steel Corporation, 20-1 Shintomi, Futtsu, Chiba-Ken, 293-8511, Japan

Abstract The influence of continuous or impulse welding current cycle on the fatigue strength of spot welded lap shear specimens is studied. The analysis of the damage mechanism and the fatigue behaviour of the spot welds are based on three experimental investigation techniques. The Potential Drop Method, the fracture surface observation and the metallographic exam contribute to the fatigue damage analysis of tested spot welds. The so called welding range has no influence on the spot weld fatigue resistance. On the contrary the welding cycle pattern and the weld time are the determinant parameters that may strongly improve the spot weld fatigue strength relatively to the welding cycle recommended by the ISO 18278-2:2004 standard. The present study is performed on a dual-phase steel homogeneous assembly.

1 INTRODUCTION

The High Strength Steels (HSS) are more and more commonly used as current grade for automotive structures. The optimization of their in use properties, as the fatigue strength is thus necessary. According to car manufacturers, 70% of the in service failures concerning the car body components are connected to joints. Among all the automotive joining techniques, spot welding is the process which is the most commonly used. Using robotics, it is fast, reliable and not very expensive. For example, there are about 3000 spot welds for the assembly of a small car body. As a consequence the understanding of the fatigue failure of spot weld is a relevant point of their fatigue behaviour assessment.

The aim of the present investigation is to show the effect of the welding current pattern on the fatigue resistance of spot welds, and to understand in which way it influences their fatigue strength through the use of accurate observation tools. A potential drop method enables to track the crack, the fracture surface examination gives information on fatigue failure damage mechanism and crack path, and microstructural zones are identified thanks to metallographic exams. Various welding patterns are thus tested. The effect of the current level, the welding cycle and the weld time are investigated and analyzed in this paper.

2 INVESTIGATION TOOLS

The whole fatigue life up to failure is not efficient enough to explain and assess the fatigue strength of single spot welded assembly. In order to clearly distinguish the mechanism of fatigue damage, investigation tools are developed, such as a crack system tracking during the fatigue test, the fracture surface observation and the metallographic analysis. These observations are then correlated to make emerge the relevant information for the analysis and the understanding of the fatigue testing results. The study is performed on a homogeneous assembly made of 600DP steel submitted to a tensile-shear loading.

2.1 Different stages of fatigue damage

The fatigue failure of Tensile-Shear spot weld Specimen (TSS), defined according to ISO 14234 :2003 [1], typically starts with a multiple cracks initiation within the Heat Affected Zone (HAZ) near the notch root between the two steel sheets. Then macro-cracks propagate circumferentially and through the sheet thickness. The fatigue crack remains invisible during the main part of the fatigue life. McMahon *et al.* [2] underline the fact that the discussion about the fatigue life of a TSS is complicated by the lack of uniform definition of fatigue life stages. Nevertheless, the fatigue life is usually divided into three steps, defined by Wang *et al.* [3]. This definition is used in the present paper to describe and track the spot-weld fatigue damage:

- Stage I: initiation and early crack growth. A detectable crack exists at the periphery of the weld nugget at the end of stage I.
- Stage II: crack propagation from the periphery of the nugget and through the thickness of the sheet.
- Stage III: crack propagation laterally across the specimen width until failure.

Many criteria exist to determine the fatigue test cut-off: loss of stiffness, plastic instability, first appearance of a surface crack, etc. Swellam *et al.* [4] noticed that a practical definition of TSS fatigue failure is the end of stage II, because the crack becomes visible on the external side of the TSS. The difficulty dwells on identifying the switch between stage I and stage II. Several methods were developed to distinguish these two stages. One solution is to stop the fatigue test at regular intervals and to make a micrograph observation. This is a destructive method that requires a good repeatability because of the fatigue failure scatter. Another technique developed by McMahon *et al.* [2], uses a specific pre-sectioned specimen allowing to track and measure the crack growth by visual observation. As the local load is modified in this case, a calculation is needed to obtain the equivalent loading. Other test methods allow to track and measure the crack directly on the specimen during the test. These techniques are all based on the similar principle: the fatigue crack growth is deduced from the change of the measured signal.

Strain gauges are used by Abe and Satoh [5], to observe the variation of the offset strain, Xu *et al.* [6,7] used the thermometry method with thermocouple, Gero [8] applies an acoustic-ultrasonic method, Cooper and Smith [9,10], Swellam *et al.* [4], and Duchet [11,12] used an electrical potential technique to monitor the crack initiation and growth through thickness. They interpret the change in the corrected potential measurement to be due to the growth of the intrinsic crack. One has to notice that the detection accuracy of each stage depends on the technique.

2.2 Potential Drop Method measurement

The Potential Drop Method (PDM) was selected in this study as the mean to determine the different stages of the spot welded fatigue life. The PDM technique is widely used for the case of planar crack to determine the fatigue crack length [13]. A high level current (alternative or direct) goes through the specimen during the fatigue test and the resulting voltage around the spot weld is measured from one sheet to the other one. The change in output voltage correlates the length of the crack and its growth during the test. In tensile-shear spot welds specimens, developed cracks do not remain planar. Nevertheless the PDM is used here to distinguish the different stages of fatigue life by the identification of crack growth rate modifications which correspond to the slope changes of the DDP versus the number of cycles.

The PDM is implemented on the TSS with a Direct Current (DC) system. Four potential drop probes are discharge-welded: two probes at about 2 mm away from the spot weld indentation, close to the expected crack position, and the two other ones on each side of the indentation surface. With this kind of measurement system both cracks initiating on the TSS can be observed separately. In addition crack initiation and growth are distinguished.

Fatigue tests on spot weld specimens were stopped at various numbers of cycles, i.e. life ratios. Micrographic exams were then performed to measure crack length. These data were then correlated to the change in voltage to express the response curves in terms of damage stages. The first change of the slope corresponds to the end of the crack initiation (stage I). The second change of slope (with a sharp edge) coincides with the first crack reaching the outer surface of the sheet. This is the end of stage II. The response feature obtained on a reference spot-weld matched typical crack growth: the initiation stage is about 30% of the fatigue life and the crack length reach the thickness at about 70%. Thus the macro-propagation phase (stage II minus stage I) is about 40% of the whole specimen fatigue life.

2.3 Fracture surface observation with SEM

In the literature, few fracture surface studies are raised and no description of the fracture surface is clearly notified [14] because of the fact that the fracture surface is not usual and may vary depending on the current level. However, a description of the different areas of the spot weld fracture surface and the information it brings are detailed in this section. This investigation campaign is based on several specimens made of 600DP 1.2mm thickness, for a 10^5 cycles fatigue life until complete failure. The main features of the fatigue fracture surface are described (see figure 1).

Many different zones are identified on a fatigue-tested TSS. The top metal sheet (1) crossed by the crack, the bottom sheet (2) and also the indentation (6) have to be noticed. The fatigue crack initiates (stage I) in the vicinity of the notch (3), then crosses the sheet through the thickness (stage II) and creates the main zone of the circumferential fracture surface (4) until the outer surface of the top sheet. At last, the crack propagates through the width of the TSS until the total failure of the specimen (stage III) and brings the secondary zone of the fracture surface (5).

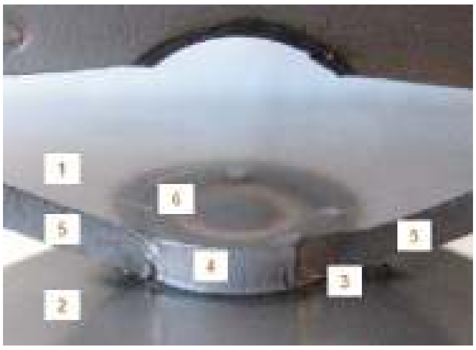

Figure 1. Particular zones of the spot weld fatigue failure surface.

The notch can be observed by two ways: facing the spot or from the side. A SEM observation enables to characterize the non-planar surface circumferentially around the spot. This observation is not possible through micrographic exams, as only one cross section is viewable with this method. It enables to make a link between the location of the fracture crack and the shape of the notch. The beginning of the specimen failure takes place at the so-called “main initiation zone”. This is the location of the fatigue crack initiation close to the notch root at the bottom of the fracture surface (zone 3 in figure 1). No fatigue striation is visible on the fracture surface, compared with typical fatigue ones for ferritic structures. In the neighbourhood of the notch root, many steps are present. They are the sign of multiple cracks initiations. Indeed, multiple cracks have initiated at the notch root in different planes (see figure 2). Then, the cracks join each other, to create a larger crack. As a matter of fact the steps are the physical marks of the joining of two cracks, as the intersection of two planes results in one straight line.

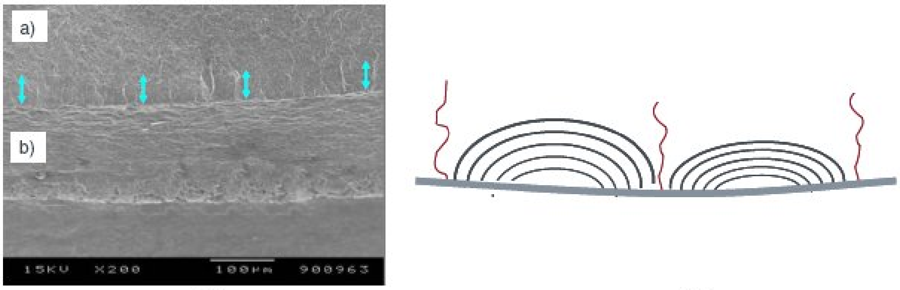

Figure 2. 1) Main initiation zone a) fracture surface b) notch root and
2) scheme of the multiple initiation site

As a consequence two fatigue cracks have initiated on both side of one step. Cooper and Smith [10] underline the difficulty to measure the first stages of the crack initiation because it remains invisible during the main part of life duration. They add that they experienced difficulties in beach-marking and fracturing specimens with cracks smaller than 220 microns [9]. Nevertheless, an oxidizing treatment has been performed to beach mark the crack at the end of the initiation stage. It shows that the average step length observed on the fracture surface corresponds to the initial length of the macroscopic crack and concurs with the slope change on the PDM measurement during the fatigue test. The upper part of the fracture surface reveals the zone crossed by the crack just before it reaches the top of the steel sheet. As for the main initiation zone, no fatigue striation appears. This is probably due to the quenched microstructure underneath, mainly martensitic. However, the details are finer for the upper part of the fracture surface than for the lower part of it. The crack has crossed in fact different microstructural zones with various primary grain sizes.

3 INFLUENCE OF THE WELD CURRENT OVER THE WELDING RANGE

The welding range of the studied steel grade is the preliminary investigation of this paper..

3.1 Base material

The high strength steel used for this study is the bare cold rolled 600DP grade from ArcelorMittal with a thickness of 1.2 mm. The chemical composition and the mechanical properties in the transverse direction (20 x 80 mm ISO specimen) are provided in Table 1.

Table I. Chemical composition and mechanical properties of 600DP steel grade.

Composition (10^{-3}%)			Yield stress (MPa)	Ultimate tensile stress (MPa)	Elongation (%)
C	Mn	Si			
Max 140	Max 1600	Max 400	360	650	> 21

3.2 Welding range

The welding range, according to ISO 18278-2 :2004 standard [15], corresponds to the Root Mean Square value range of the current when all the other welding parameters are fixed. For this thickness and steel grade in homogeneous assembly, the conditions are:

- electrode type : TH6
- electrode force: 4000 N
- welding time: 14 periods
- holding time: 14 periods

The lower limit of the welding range corresponds to the RMS value for a 4 mm minimum nugget diameter. The expulsion or splashed point defines the higher limit of the current range.

The mechanical strength is usually performed for Cross-Tension Specimen (CTS) or Tensile-Shear Specimens (TSS). For both loading mode, the mechanical strength is improved with the increasing of the current value. The mechanical strength remains nevertheless constant for splashed point. The general trend is that the nugget diameter, the corona bond diameter and the sheets separation increase with the current level. In terms of notch root shape, the edge is very sharp for a low current level, the greater the RMS current is and the smoother the edge is. However for splashed point, the notch is very sharp because of the expelled metal particle between the faying surfaces.

3.3 Effect on the fatigue behaviour

In order to reduce the scatter and improve the reliability of the results, all the specimens were prepared during the same experimental welding campaign. The TSS are then tested under constant amplitude fatigue loading (maximal loading of 3000 N with a 0.1 load ratio), with a geometry defined by ISO 14234:2003 standard [1] on a servo-hydraulic fatigue machine. All the tests are implemented with PDM measurements. The displacement limit of the actuator is the test end criterion.

Barkey and Zhang [16] summarise three main approaches to assess the fatigue behaviour of weld spots. Firstly, the load-life analysis considers the load as the basic damage parameter. A stress intensity approach based on fracture mechanics was developed by Pook [17], Smith and Cooper [18], Zhang [19] and Radaj [20]. The structural stress approach was considered by Rupp *et al.* [21], Radaj *et al.* [22]. According to Rupp *et al* [21] the latter method is an efficient way in an engineering sense to assess the fatigue of spot welded structure, and it is the most implemented method in the software used by car manufacturers. It enables to localize the weakest point of a structure in term of fatigue damage and to predict the failure mode. Two failure modes may be assessed: a cracking through the weld nugget, i.e. interfacial failure, and a cracking in the metal sheet. One has to notice that only geometrical parameters are taken into account in this method.

The figure 3 shows the experimental results expressed as the whole life for the constant amplitude fatigue loading described above. The button diameter value is calculated thanks to the RMS current value. Since the nugget is well developed, i.e. bottom of the welding range, the crack through thickness failure mode is observed. Then, no significant evolution of the number of cycles is noticed until a high level of current over expulsion. In these cases, large distortions are observed on specimens.

The structural stress approach generally predicts some improvement of the fatigue behaviour when the current level increases as the nugget diameter is getting higher simultaneously. The experimental results show that this trend is not verified over the welding range.

The observation of the fracture surface indicates two different starting point of the fatigue crack depending on the current level. The crack initiates generally from the notch root and propagates through the fine Grain Heat Affected Zone except for low current level where a corona bond zone exists and fails immediately just after several fatigue cycles.

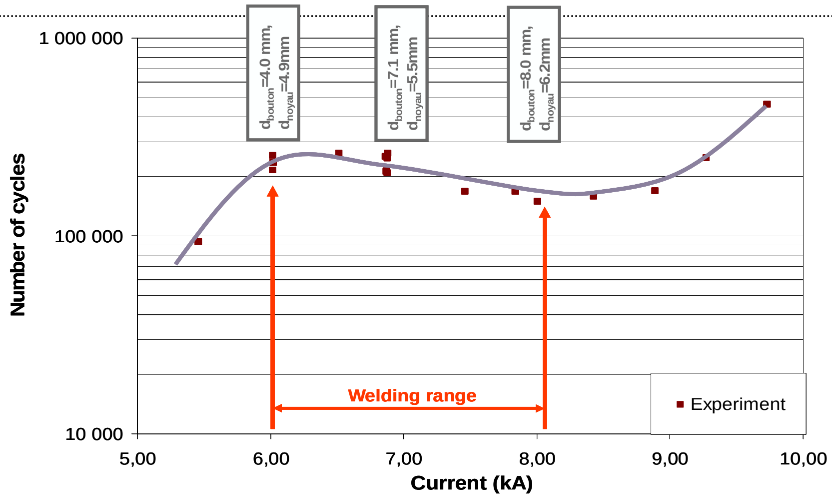

Figure 3. Fatigue life up to complete failure versus current level (maximum load equal to 3000 N and 0.1 load ratio).

4 INFLUENCE OF THE CURRENT PATTERN

The effect of the current pattern of the welding cycle is investigated in this section. The first study concerns the formation of the nugget. The nugget size is defined by its width and its thickness. Monotonic mechanical properties are determined for the reference welding cycle provided by the ISO 18278-2 :2004 standard [15] and for other current patterns. All the specimens have been welded on a pedestal welding machine with a 50 Hz frequency and during the same experimental campaign. Two kinds of welding cycle patterns are investigated:

- Simple spot welding feature: the current flow passes through the specimens during one sequence which duration is analysed here.
- Pulsation spot welding feature: the current flow is delivered during several sequences separated by hold times.

4.1 Nugget formation

All the welding parameters are settled similar: the electrode force is 400 daN, the TH6 electrode type is chosen and the target current value corresponds to the middle of the welding range defined by the ISO 18278-2 :2004 standard. To ensure a usual welding process, the evolution of the dynamic resistance curve versus the weld time is compared to the definition made by Dickinson *et al.* [23] and to Gedeon and Eagar [24]. It matches a typical evolution for a bare steel. The different geometrical dimensions of the weld are measured on cross-sectioned samples, which are etched with Bechet-Beaujard reagent [25]. The diameter and penetration of the nugget are shown in figure 4. They are plotted as functions of weld time (expressed in periods) for the case of continuous pattern. The observed trends are in good agreement with the results of Cho and Cho [26] for a 1.6 mm thickness mild steel. Once the melting has begun, the nugget expends in all directions and goes in a steady-state at first for the nugget penetration (thickness) after 2 or 3 periods since melting, and after 10 periods concerning the nugget diameter. William and Parker [27] observe a similar phenomenon in case of thin sheet welding. Since the initiation of a molten zone, almost 90% of the total weld growth occurred during the next 2-4 cycles of current flow. Moreover Cho and Rhee [28] observed the nugget formation mechanism by the use of a high speed camera, and noticed that the nugget oscillates with twice the frequency and that its size tends to be saturated.

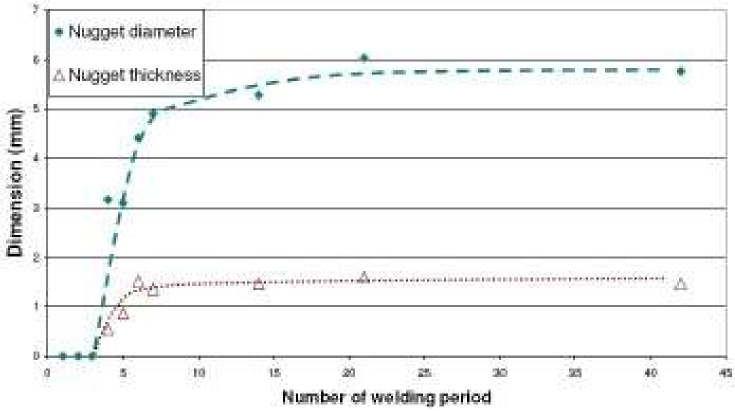

Figure 4. Thickness and diameter of the nugget spot weld versus welding time in the case of continuous welding cycle pattern

In comparison with the Nital etching that reveals the martensitic structure and gives the maximal nugget size, the Bechet-Beaujard reagent enables to reveal the primary austenitic structure. The optical micrographs show the last solidification front (figure 5). The longer the weld time is and the smallest the last melted zone is. The nugget formation mechanism is easily depicted. The melting occurs after few periods of current flow. The nugget expends in all directions, stabilizes its penetration and its diameter, and then the liquid zone volume begins to decrease. For a multi impulse current, the different melted zones boundaries can be identified also easily. At the first current pulse, the constituted melted zone has the maximal penetration, the second pulse makes increase the diameter of the melted zone. During the last impulse, the melted volume is the smallest one. There is neither increase of the nugget thickness nor any rise of its diameter. The same mechanism is observed and its influence is greater when using a cool time. This phenomenon is of course sensitive to the RMS value and to the sheet thickness.

a)

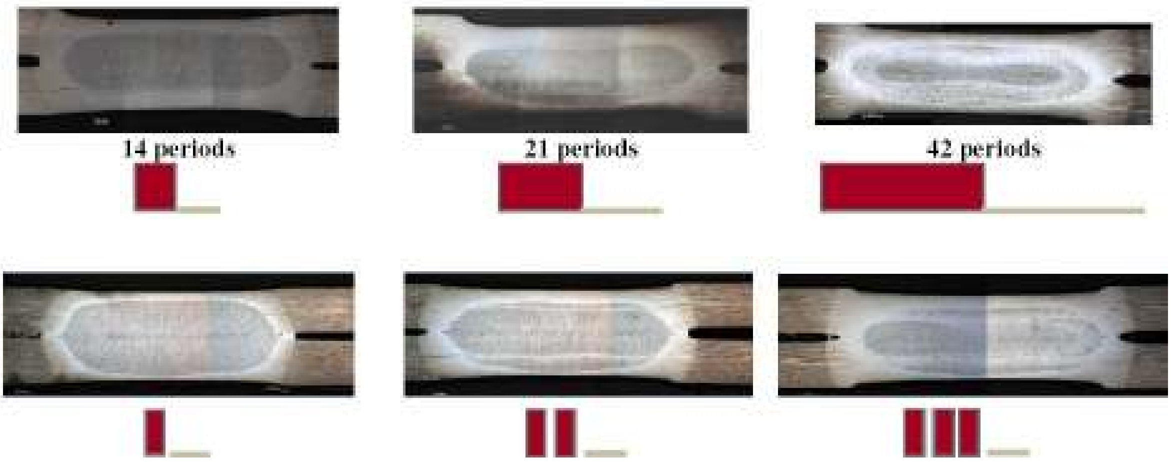

b)

Figure 5. Optical micrograph of the cross section of the spot weld in case of a) continuous welding pattern b) multi impulse welding pattern

4.2 Influence of the current pattern on monotonic mechanical properties

The welding current patterns and their symbols are summarized in table 2. All the other welding conditions are settled similarly and are defined from ISO 18278-2 :2004 standard. The target current value corresponds to the middle of the welding range defined before. In the case of long weld time, i.e. C28 and C42 conditions, the hold time is settled also longer to avoid the determination of an adequate hold time which is experimentally time consuming. By this way it is for sure that the assembly is cold enough and that the microstructure is fixed.

Table II. Definition of the welding current patterns.

Welding conditions case	Current pattern feature	Welding cycle (number of flow current periods)	Hold time (number of periods)	Symbols
Reference	continuous	14	14	
P3	multi-impulse	3 x (7+2)	15	
P4	multi-impulse	4 x (7+2)	15	
C21	continuous	21	14	
C28	continuous	28	28	
C42	continuous	42	42	

Figure 6 shows the ratio of the mechanical strength in Cross-Tension and Tensile-Shear loading over the one obtained for the reference condition. Three specimens are used in each case to calculate the mean value. For the CT tests, the reference condition exhibits the best behaviour. For the continuous welding cycle, the weld time increase leads to a decrease of the CT strength. The opposite effect is observed in TS loading. No improvement is observed for a multi impulse current.

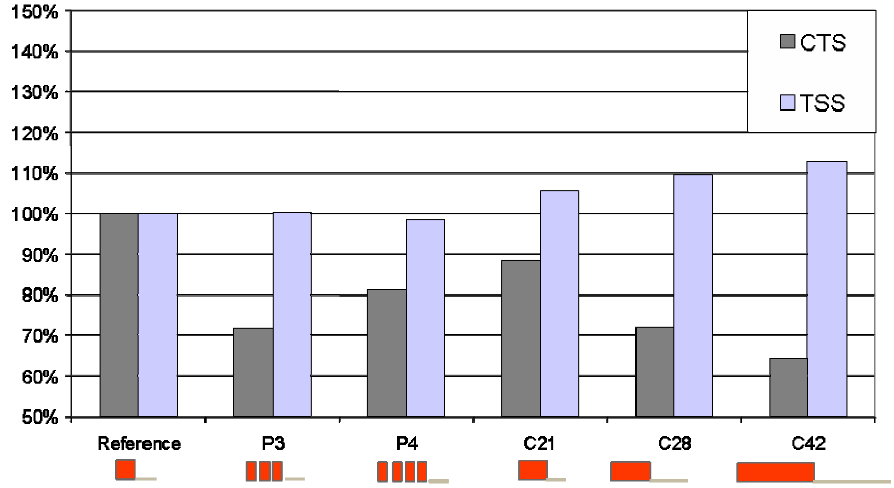

Figure 6. Effect of the current pattern on the monotonic mechanical strength under tensile-shear and cross tensile loading

4.3 Influence on the fatigue behaviour

For these welding conditions, the TSS are tested in fatigue (maximal loading of 3000 N with a 0.1 load ratio). For the condition C42, no specimen has failed at 3000 N. So another fatigue loading is applied to the same set of specimens, with a maximal loading equal to 4000 N and still the 0.1 load ratio. All the tests are implemented with PDM measurements. The maximum displacement of the actuator is the test end criterion. Five specimens of each batch are tested in order to obtain some efficient statistical confidence on the mean life. The distribution law of the fatigue life is assumed to be logarithmic-normal. The different stages of fatigue damage are measured with the PDM and are detailed on figure 7. As a result the improvement of the whole lifetime results from the rise of the initiation stage life. Concerning the stage II, it is important to notice that the mean propagation durations for five batches tested at 3000 N are similar and are about 6.10^4 cycles. Considering the confidence interval, the mean life of the macro-crack propagation (stage III) is not statistically different. Moreover, by using the analysis of variane (ANOVA) on the propagation life based using the Fischer-Snedecor law [29], the equivalence assumption can not be rejected. Considering the confidence interval at 95% of the initiation stage, only condition C28 is not equivalent. The difference in terms of fatigue life is thus statistically significant.

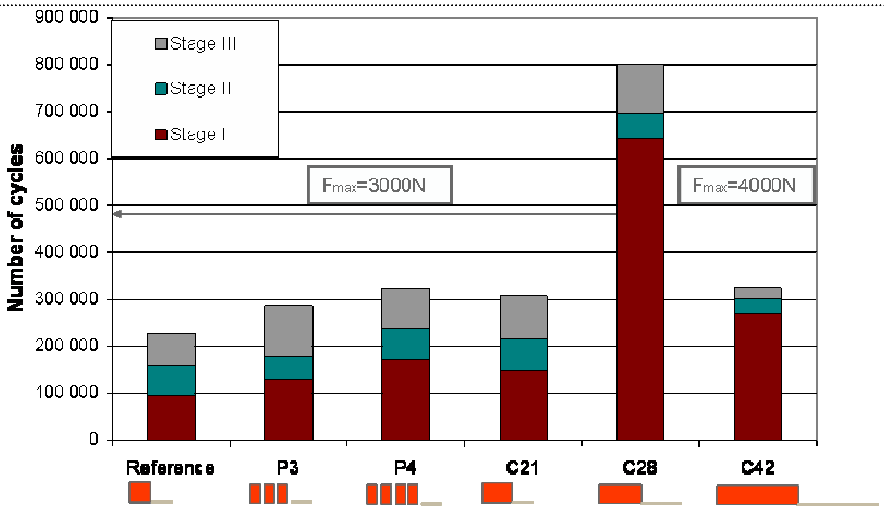

Figure 7. Fatigue lives corresponding to the three damage stages versus the welding cycle pattern

4.4 Improvement of the admissible fatigue loading

In order to quantify the improvement in terms of applied load, an equivalent load estimated from the mean lives of each batches is estimated. The assumption that the slope of the "Load / Number of cycles to initiation" Basquin curve is the same for all the welding conditions has been used. The ratio of the calculated equivalent loading on the reference condition one is shown in figure 8. The multi-impulse current pattern induces more than 10% improvement for the mean value, which is not statistically significant considering the fatigue scatter. It is worth to note that the increase of the number of impulses generates a rise of the fatigue strength. In the case of continuous current cycle, the fatigue strength strongly increases with the weld time up to 40%.

The continuous pattern shows a better fatigue behaviour than the multiple impulses one. The hold time is not taken into account here but, as written above, for C42 and C28 welding conditions, the hold time could be stated shorter. As a conclusion, the improvement of fatigue strength is strongly linked to the weld time and to the current pattern. In all cases, this improvement is mainly due to the increase of initiation stage.

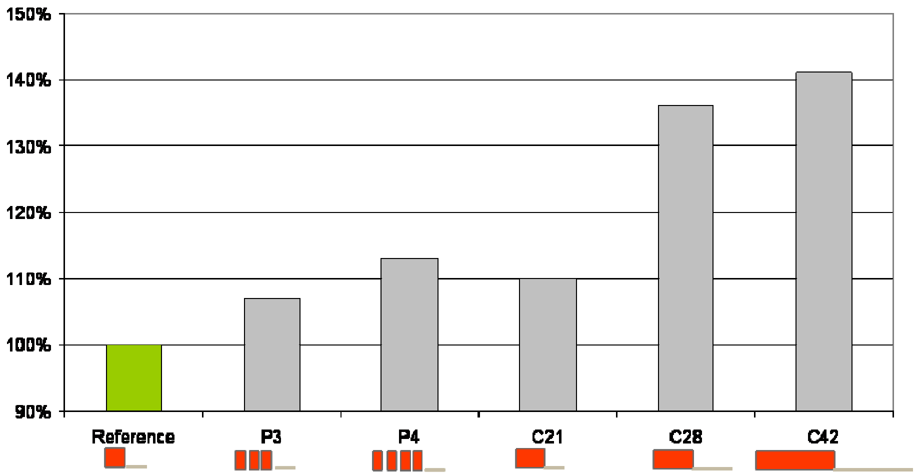

Figure 8. Fatigue resistance improvement on initiation stage in terms of maximum admissible load ratio versus the welding cycle pattern

5 CONCLUSION

The purpose of the present paper is to analyze the influence of the welding cycles on the fatigue resistance of spot welded lap shear joints subjected to tensile-shear loading. The effect of the welding pattern on spot welded High Strength Steel 600DP is quantified. Over the welding range, despite the increase of the nugget diameter generated by the current level growing, no significant difference on fatigue life is observed. Two different mechanisms are identified for the initiation stage and explain this similar fatigue behaviour. By changing the welding pattern and especially the weld time, an outstanding fatigue strength improvement is obtained. This is mainly due to the increase of the initiation stage.

Considering the weld time, the benefit of continuous pattern is clearly underlined. These results are obtained by the use of accurate methodology and observation tools which are fundamental to understand the fatigue damage mechanism as well as the nugget formation. The Potential Drop Method (PDM) implemented on fatigue specimens, the fracture surface observations and the metallographic analysis are efficient and complementary tools by the information they provide about the fatigue failure. These different techniques were developed for a homogeneous 600DP steel grade assembly and can be easily extended and applied to other high strength steel grades.

6 REFERENCES

1. ISO 14234 :2003 Soudage par résistance- Essais destructifs des soudures- Méthode pour les essais de fatigue sur les assemblages soudés par points.
2 J.C. MacMahon, G.A. Smith and F.V. Lawrence, Fatigue and Fracture Testing of Weldments, ASTM STP 1058, H.I. Mac Henry, J.M. Potter, Eds., American Society for Testing and Materials, Philadelphia, 1990, 47-77.
3. P.C. Wang, H.T. Corten and F.V. Lawrence, SAE Technical paper 850370, Society of Automotive Engineers, Warrendale, P.A., 1985.
4. M.H. Swellam, P. Kurath and F.V. Lawrence, Advances in Fatigue Lifetime Predictive Techniques, ASTM STP 1122, M.R. Mitchell and R.W. Landgraf, Eds., American Society for Testing and Materials, Philadelphia, 1992, 383-401.
5. H. Abe and T. Satoh, *Welding International*, 7 (1), 1993, 35-41.
6. P. Xu, B. Lehmkuhl, DVM-Tagungsband Kennwertermittlung für die Praxis, Whiley-VCH Verlag, Weinheim, 2002, 211-216.
7. P. Xu, *Welding in the World*, 48(11), 2004.
8. B.M. Gero, <u>Acousto-ultrasonic evaluation of cyclic fatigue of spot welded structures</u>, Master of Science Thesis, Virginia Polytechnic Institute, 1997.
9. J.F.Cooper and R.A. Smith, *International Journal of fatigue*, 7(3), 1985, 137-140.
10. J.F.Cooper and R.A. Smith, *Metal Construction*, 1986.
11. M. Duchet, <u>Etude de la tenue en fatigue des assemblages soudés par points</u>, DESU report, Metz University, 1994.
12. M. Duchet, F. Rossillon, A. Galtier, M. Landy and E. Easterbrook, *Welding in the world*, to be published.
13. B. Marandet, G. Labbe, J. Pinard and M. Truchon, IRSID, RE549, June 1978
14. M. Vural, A. Akkus and B. Eryürek, *Journal of Materials Processing Technology*, 176, 2006, 127-132.
15. ISO 18278-2 :2004 Soudage électrique par résistance- Caractérisation de la soudabilité par résistance par point de produits plats revêtus ou non.
16. Y.L. Lee, J. Pan, R. Hathaway and M. Barkey, <u>Fatigue Testing and Analysis - Theory and Practice</u>, M. Barkey and S. Zhang, Chap 7 - Fatigue of spot welds, Elsevier, 2005.
17. L.P. Pook, *International Journal of Fracture*, 11, 1975, 173-176.
18. R.A. Smith and J.F. Cooper, Fatigue of Welded Constructions, The Welding Institute, Abington, Cambridge, 1988.
19. S. Zhang, *Welding Journal*, 78, 1999, 173-179.
20. D. Radaj, *Engineering Fracture Mechanics*, 34, 1989, 495-506.
21. A. Rupp, K. Stoerzel and V. Grubisic, SAE Technical Paper 950711,Warrendale Pa, SAE, 1995.
22. D. Radaj and C.M. Sonsino, <u>Fatigue assessment of welded joints by local approaches</u>, Abington Publishing, 1998.
23. D.W. Dickinson, J.E. Franklin and A.Stanya, *Welding research supplement*, 59 (6), 1980, 170-176.
24. S.A. Gedeon and T.W. Eagar, *Metallurgical transactions*, 7B, 1986, 887-901.
25. S. Bechet and L. Beaujard, *Revue de Métallurgie*, 10, 1955, 1045-1052.
26. H.S. Cho and Y.S. Cho, *Welding Research Supplement*, 1989, 236-244.
27. N.T. Williams and J.D. Parker, *International Materials Reviews*, 49 (2), 2004, 45-75.
28. Y. Cho and S. Rhee, *Welding Journal*, 2003, 195-201.
29. NF ENV 130005, 1999.